Parametric Polar Maps of Regional Myocardial β-Adrenoceptor Density

Richard M. de Jong, Christopher G. Rhodes, Rutger L. Anthonio, Antoon T.M. Willemsen, Paul K. Blanksma, Adriaan A. Lammertsma, Stuart D. Rosen, Willem Vaalburg, Harry J.G.M. Crijns and Paolo G. Camici

Department of Cardiology/Thorax Center and PET Center, Groningen University Hospital, Groningen, The Netherlands; MRC, Cyclotron Unit, Imperial College School of Medicine, Hammersmith Hospital, London, England

Quantification of myocardial β-adrenoceptor density (B_{max}) is of interest in cardiac diseases in which altered function of the sympathetic nervous system is thought to play a pathophysiological role. PET provides an unrivaled means of taking regional measurements of cardiac microcirculatory function, tissue metabolism and autonomic nervous system activity. Measurements in small regional areas may be biased because of increased noise levels. This study examined the parametric polar map approach for the regional quantification of B_{max}. **Methods:** Dynamic PET with parametric polar map imaging was performed in 10 healthy volunteers and 4 patients with hypertrophic cardiomyopathy using (S)-[^{11}C]-(4-(3-tertiarybutylamino-2-hydroxypropoxy)-benzidimazole-2)-on hydrochloride (CGP)-12177 and a double-injection protocol. Time-activity curves were corrected for partial volume, spill-over and wall motion effects. The mean B_{max} of the left ventricle was calculated in two ways. First, the average time-activity curve of all segments, having the highest achievable signal-to-noise ratio, was used to calculate $B_{max(mTAC)}$ (the myocardial beta-adrenoceptor density of the left ventricle calculated using the average time-activity curve). The bias in $B_{max(mTAC)}$ introduced by noise is minimal. Second, an estimate of whole-heart receptor density was calculated using the polar map method by averaging the values of B_{max} obtained for 576 individual segments. In these calculations, three different filters (3 × 5, 3 × 9 and 3 × 13 segments) were used to smooth the time-activity curves before calculating B_{max}. Mean values of whole-left-ventricular receptor density obtained by averaging regional values using the different filters ($B_{max(PMF1/2/3)}$) were compared with $B_{max(mTAC)}$ to assess bias introduced by the polar map approach. Segments with a calculated B_{max} outside the range 0.1–50 pmol/g were considered unreliable and were excluded from the analysis. **Results:** The differences between the two methods of calculating B_{max} were small (7.8%, 4.8% and 3.2%, with the three filters, respectively). Reliable results were obtained in >95% of the segments and in 9 volunteers and all 4 patients. **Conclusion:** When using PET for the quantification of β-adrenoceptor density, the regional variation in B_{max} can be reliably assessed using the parametric polar map approach.

Key Words: β-adrenoceptor; PET; parametric imaging

J Nucl Med 1999; 40:507–512

Received Mar. 19, 1998; revision accepted Sep. 15, 1998.

For correspondence or reprints contact: Richard M. de Jong, PhD, Department of Cardiology/Thorax Center, Groningen University Hospital, P.O. Box 30001, 9700 RB Groningen, The Netherlands.

Local variation in values of myocardial β-adrenoceptor density (B_{max}) may be of interest in cardiac diseases in which altered function of the sympathetic nervous system is thought to play an important pathophysiological role. These include hypertrophic cardiomyopathy and ischemic and arrhythmogenic heart disease. Regional measurements may provide a better understanding of the underlying pathophysiology and the efficacy of various treatment regimens (*1*). Using in vitro binding assays, changes in B_{max} have been recorded in many cardiac diseases (*2*), specifically congestive heart failure (*3*), myocardial ischemia (*4*), cardiomyopathy (*5*) and valvular disease (*6*). Furthermore, changes of B_{max} have been associated with hypertension (*7*), diabetes (*8*), hyperthyroidism (*9*) and chronic drug administration (*10*). Regional variation of the sympathetic function of the heart may be expected in coronary artery and arrhythmogenic heart disease (*11*), diabetic cardiac neuropathy (*12*) and during the process of reinnervation after heart transplantation (*13,14*). Measurement of cardiac receptor density using in vitro binding assays, however, requires myocardial biopsies or autopsy material, making regional information difficult to obtain and repeated measurements impossible to perform. PET allows local quantification of isotope concentration to be made in vivo, providing an unrivaled noninvasive means of performing regional measurements of cardiac microcirculatory function, tissue metabolism and autonomic nervous system activity (*15*). Using PET and the nonselective β-antagonist radioligand (S)-[^{11}C]-(4-(3-tertiarybutylamino-2-hydroxypropoxy)-benzidimazole-2)-on hydrochloride (CGP)-12177, it is possible to measure B_{max} noninvasively in the left ventricle (*16–23*). This provides regional information with the ability to perform repeat measurements and obtain data in healthy volunteers.

However, a problem associated with PET measurements in small regions is the potential for biased results because of lower signal-to-noise ratios (*24*). The first studies using PET and ^{11}C-CGP reported down-regulation of β-adrenoceptors in the left ventricle of patients with idiopathic dilated (*18*) and hypertrophic (*19,21*) cardiomyopathies. In these studies, the ability of PET to obtain regional information was not fully exploited; for example, heterogeneity was studied by

Lefroy et al. (*19*), by obtaining values of B_{max} from only 20 segments in the left ventricle.

The aim of this study was to investigate the effect of bias in the measurement of regional B_{max} in small areas of the left ventricle using the parametric polar map approach. Scan data collected for some of the studies previously reported (*19,21,23*) were used in this analysis for obtaining a range of low to high values for B_{max}.

MATERIALS AND METHODS

Population

Four patients with hypertrophic cardiomyopathy (3 men, 1 woman; 55 ± 6 y) and 10 healthy volunteers (5 men, 5 women; 53 ± 12 y) were studied after a 6-h fast. A 21G cannula was inserted into a forearm vein for the infusion of tracers. Blood pressure and electrocardiogram were recorded at 10-min intervals throughout the study. All subjects gave written informed consent to a protocol approved by the Hammersmith Hospital Research Ethics Committee and the United Kingdom Administration of Radioactive Substances Advisory Committee.

PET Scanning

The subjects were positioned on the couch of an ECAT 931–08/12 15-plane positron tomograph (CTI/Siemens Inc., Knoxville, TN), and the heart was positioned in the center of the field of view using a short rectilinear transmission scan. A 20-min transmission scan was performed using retractable circular ring sources, each filled with ~ 74 MBq (2 mCi) ^{68}Ge. Regional blood volume was then measured by inhaling ^{15}O-labeled carbon monoxide (C^{15}O). One minute after the C^{15}O inhalation (a 4-min gas delivery at a flow of 500 mL/min and a radioactive concentration of 3.0 MBq [0.08 mCi]/mL), a 6-min static emission scan was performed. Four serial venous samples were taken during this scan and counted in a well counter cross-calibrated with the scanner. Finally, a dynamic β-adrenoceptor scan was acquired using the double-injection protocol described by Delforge et al. (*16*). A first dose of ^{11}C-CGP (4.2 ± 0.4 μg, 156 ± 28 MBq [4.2 ± 0.8 mCi]) was followed 30 min later by a second dose (24.3 ± 1.8 μg, 330 ± 58 MBq [8.9 ± 1.6 mCi]). Both doses were infused over a 2-min period. The dynamic scan comprised 55 frames, the first, a 30-s background frame, followed by 24 frames (8 × 15, 4 × 30, 2 × 60, 2 × 120, 8 × 150 s) acquired after the first injection and an additional 30 frames (8 × 15, 4 × 30, 2 × 60, 2 × 120, 14 × 150 s) acquired after the second.

Data Analysis

Sinograms were normalized, attenuation corrected and reconstructed to provide dynamic images with a transaxial spatial resolution of 8.4 mm full width at half maximum (FWHM) and a slice thickness of 6.6 mm FWHM.

Parametric images of blood volume (V_B, mL/mL region of interest [ROI]) were acquired by relating equilibrium images of the C^{15}O distribution to the radioactivity concentration of venous blood samples obtained during the scan. Parametric images of extravascular density (D_{EV} [g/mL ROI]) were acquired by normalizing the transmission (TR) scan to determine the tissue density distribution (g/mL ROI). This was achieved by dividing the transmission image by the mean pixel count from a vascular ROI in the chamber of the left ventricle (ROI_{TR_LV}) and multiplying by the value for the density of blood (1.06 g/mL, Geigy Scientific Tables). This relies on the known linear relationship between pixel counts in the transmission image and physical density (*24*). Extravascular density was determined by subtracting vascular density (1.06V_B [g blood/mL ROI]) from the density distribution (*24,25*), thus

$$D_{EV} = 1.06 - [(Tr/ROI_{TR\_LV}) - V_B].$$

The dynamic ^{11}C-CGP frames were corrected for decay, and a static ^{11}C-CGP image was created by summing the frames from 6–30 min. This image was used to define the axis for re-orientation and for myocardial delineation. All images were re-oriented to 12 myocardial short-axis slices and analyzed using a modification of the parametric polar map method described by Blanksma et al. (*26*). The myocardial areas in the short-axis slices were defined by two concentric circles to delineate the inner (endocardial) and outer (epicardial) surfaces. The myocardium was then circumferentially divided into 48 segmental ROIs within each slice. Time-activity curves were generated for all ROIs, resulting in a total of 576 curves. To obtain the appropriate values of blood volume and tissue density for each region, the same ROIs were applied to the V_B and D_{EV} images. Blood activity was assessed using small circular regions drawn in the left atrium. Time-activity curves from each of the ROIs applied to the dynamic ^{11}C-CGP scan were corrected for spill-over (^{11}C-CGP blood background) and partial volume effects (wall thickness and wall motion) using the values of D_{EV} and V_B determined for the corresponding regions using the equation:

$$C_t = [C_m - (V_B \times C_{LA})]/D_{EV},$$

where C_t and C_m denote the ^{11}C-CGP concentrations in myocardial tissue (Bq/g) and the myocardial ROIs (Bq/mL ROI), respectively. C_{LA} denotes the vascular ^{11}C-CGP concentration obtained from the left atrial ROI (Bq/mL blood). The blood component V_B is assumed to be arterial. This is reasonable because it is dominated by arterial spill-over from the left ventricular blood pool (*27*). Normal myocardial blood volume is approximately 12%, of which approximately 4% is arterial. In addition, the single pass extraction of ^{11}C-CGP is thought to be low (≤20%, Rhodes et al., unpublished data, 1995), resulting in similar venous and arterial concentrations. The concentration of ^{11}C-CGP bound to β-adrenoceptors after each injection was assessed using a logarithmic curve fit between 10 and 30 min and between 40 and 75 min. β-adrenoceptor density (pmol/g) was calculated between the limits 0.1 and 100 pmol/g using the concentrations obtained by the fitting procedure and the injected doses as described by Delforge (*17*).

Polar Map Calculations. Before the value of B_{max} for each ROI was calculated, time-activity curves were filtered using the data in the surrounding regions. Three different filters were used to assess regional B_{max}:

Filter 1. Time-activity curves from 3 × 13 ROIs were averaged for all segments except those at the apical or basal boundary of the heart, where 2 × 13 segments were averaged.

Filters 2 and 3. Time-activity curves were averaged from 3 × 9 (or 2 × 9) segments and 3 × 5 (or 2 × 5) segments, respectively. Two examples of filter 2, one at the basal boundary and one midventricular, are displayed in Figure 1. Each filter was based on averaging the time-activity curves of the segment of interest and the surrounding segments, using equal weighting factors for all segments. The segments with a calculated B_{max} outside the range 0.1–50 pmol/g were considered unreliable and were excluded from further analysis.

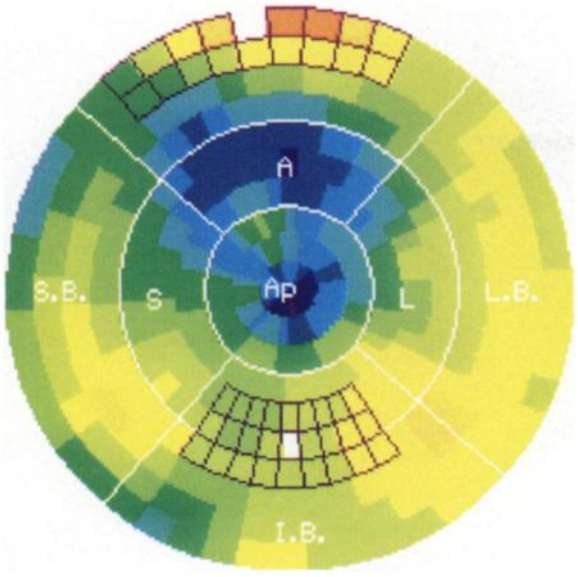

FIGURE 1. Extent of filter 2 is shown projected onto polar map of heart for basal segment (filter size: 2 × 9 segments) and midventricular segment (filter size: 3 × 9 segments). To calculate B_{max} in segment of interest (white in figure), average time-activity curve of surrounding segments (marked) and segment of interest was averaged, using equal weight for all segments. A = anterior; Ap = apical; B = basal; I = inferior; L = lateral; S = septal.

Whole Heart B_{max} Calculation. The mean left ventricular B_{max} was calculated in two ways. First, the average time-activity curve of all segments was used to calculate $B_{max(mTAC)}$. This curve has the highest achievable signal-to-noise ratio and, therefore, the minimum bias due to noise. Second, the mean B_{max} was calculated using the polar map method with the three filters ($B_{max(PMF1/2/3)}$), where B_{max} values in all accepted segments were averaged.

Values obtained with the different filters ($B_{max(PMF1/2/3)}$) were compared with $B_{max(mTAC)}$ to assess the noise-related bias introduced by the polar map approach. This difference was expressed as percentage of $B_{max(mTAC)}$.

Statistical Analysis. The results are presented as mean ± SD. Student paired *t* test was used for statistical analysis of differences between $B_{max(mTAC)}$ and $B_{max(PMF1/2/3)}$. P value < 0.05 was considered statistically significant.

RESULTS

Polar maps from two volunteer and two patient studies are shown in Figure 2. Figure 2A shows a polar map from a healthy volunteer with a homogeneous distribution of B_{max}. Figure 2B demonstrates the distribution of receptor density from a volunteer with high values in the inferior area, possibly due to spill-over from the liver. Figure 2C shows the heart of a patient with a low, homogeneous distribution of B_{max}, and Figure 2D illustrates a patient with a heterogeneous distribution of receptor density, with lower B_{max} values in the anterior and posterolateral areas. With all filters, significant differences were found between $B_{max(mTAC)}$ and $B_{max(PMF1/2/3)}$ (Table 1). The largest difference was found with the smallest filter (7.8% ± 7.3%). In all studies but one, β-adrenoceptor density could be calculated in more than 95% of the segments, even with the smallest filter. With the smallest filter, one study (volunteer 10) yielded unacceptable results in 16% of the segments.

DISCUSSION

This study examined the possibility of measuring regional myocardial B_{max} in the left ventricle with the parametric polar map approach. Acceptable results were obtained in 13 out of 14 studies. Although significant, only small differences were found between the myocardial β-adrenoceptor density calculated with a single average whole-heart time-activity curve ($B_{max(mTAC)}$) and that determined with the polar map approach ($B_{max(PMF1/2/3)}$). The values of B_{max} found for the 4 patients with cardiomyopathy were lower than the values obtained for the healthy volunteers, as previously reported (*19,21,23*). There was, however, no apparent difference in bias recorded for the two groups.

Methodological Considerations

The Parametric Polar Map Method. The parametric polar map method is a general approach that can be used for all cardiac PET studies. It has been applied successfully to studies of myocardial glucose uptake (*26*) and perfusion (*28*). This approach is compatible with the standardization and automation of data analysis and gives a clear presentation of the regional distribution of the parameter under investigation. In this study, three filter sizes and 12 myocardial slices divided into 48 segments each were used. Depending on the tracer, the model and the signal-to-noise characteristics, segments can be averaged or more complex filtering methods can be used to obtain better signal-to-noise ratios. The standardization of the number of slices has a great advantage when comparing the distribution of B_{max} (or other cardiological parameters, e.g., perfusion and glucose uptake) between volunteer and patient groups. However, a standard reorientation to 12 short-axis slices gives a variable axial thickness of the sectors between subjects, because of variation in the size of the heart. In larger hearts, the volume of a sector will be larger and could therefore give data with a better signal-to-noise ratio. Thus, the amount of bias may vary between hearts of different sizes. However, when a filter results in a low bias, the true differences in B_{max} between volunteers and patients will generally be much larger than those introduced by the polar map analysis. The division of each myocardial short-axis slice into 48 segments results in a progressively smaller volume per segment, moving from the base of the heart to the apex. Therefore, the bias in the apical region will be expected to be slightly higher than in the other regions. Division of the apical region into a smaller number of segments might solve this problem but would require a more complex spatially variable filter.

Calculation of B_{max}. When considering differences in the subjects' ages, the values of B_{max} obtained for the normal subjects in this study are, as expected, similar to those reported by Lefroy et al. (*19*), Choudhury et al. (*21*) and Rosen et al. (*22*), but are slightly higher than those reported

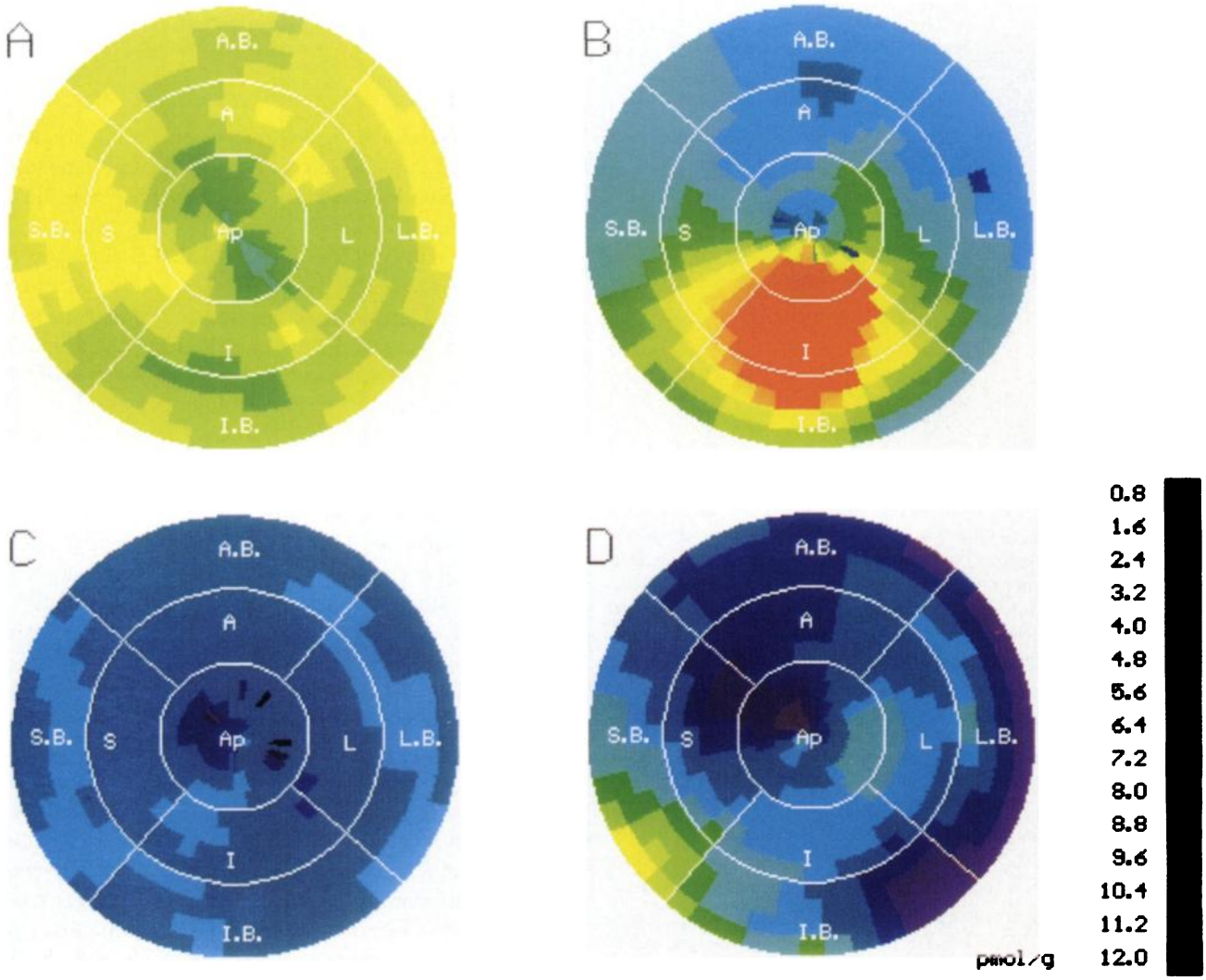

FIGURE 2. Polar maps of β-receptor density in hearts of 2 volunteers (A and B) and 2 patients (C and D) using filter 2. A = anterior; Ap = apical; B = basal; I = inferior; L = lateral; S = septal.

by Merlet et al. (*18*). This discrepancy is partly due to the subsequent improvement in the method of calculating B_{max} used by Delforge (*17*), which was the method we used from the outset. In addition, different corrections for the partial volume effect were used. Merlet et al. (*18*) used a recovery factor based on echocardiographic measurements of left ventricular wall thickness. This approach does not correct for partial volume effects arising from wall motion. Furthermore, the spill-over effect of radioactivity in the heart chambers was not considered in their calculations. In our study, tissue density and blood volume were measured to correct for partial volume effects, wall motion and the spill-over of activity from blood to tissue. The main advantage of this method is that correction factors are assessed shortly before the ^{11}C-CGP scan using the same instrumentation. A drawback is that an additional $C^{15}O$ scan is required, resulting in a higher radiation dose to the subject and a higher risk of artifact due to movement between scans.

An alternative approach to the assessment of partial volume effects would be to use the information on tissue fraction obtained from the myocardial perfusion measurements using intravenous $H_2{}^{15}O$ bolus (*25,29,30*). The main advantage of an assessment of perfusable tissue fraction is that a correction for infarcted areas is made. This allows the normalization of a given parameter to the amount of viable ($H_2{}^{15}O$ exchangeable) myocardial tissue in an ROI. This contrasts with a normalization based on extravascular density in which the parameter is expressed per gram of total tissue (i.e., viable plus scar). Although myocardial perfusion is routinely measured in most cardiac studies performed by our group, the ^{11}C-CGP protocols used here relied on myocardial perfusion measurements made using the inhalation of $C^{15}O_2$ (*27*). Because the approach is associated with erroneously high values of tissue fraction in the septum due to spill over from the right ventricle (*25*), extravascular density was used for the partial volume correction in these clinical studies. It has been shown that this problem can be overcome by using intravenous $H_2{}^{15}O$ (*30*). Ideally, such

TABLE 1
Differences Between Mean $B_{max(mTAC)}$ and Mean $B_{max(PMF)}$

Subject no.	mTAC	PMF 1 (3 × 13 segments)		PMF 2 (3 × 9 segments)		PMF 3 (3 × 5 segments)	
	mB_{max} pmol/mL	mB_{max} pmol/mL	Difference %	mB_{max} pmol/mL	Difference %	mB_{max} pmol/mL	Difference %
Patient							
1	4.4	4.5	2.6 (576)	4.6	3.9 (576)	4.8	7.3 (576)
2	4.5	4.5	−0.0 (576)	4.5	−0.0 (576)	4.6	0.8 (576)
3	4.6	4.8	2.5 (576)	4.9	5.0 (576)	5.3	13.5 (575)
4	5.5	5.9	6.2 (576)	6.1	11.3 (573)	6.6	20.4 (568)
Volunteer							
1	6.6	6.7	1.0 (576)	6.7	1.0 (576)	6.8	1.7 (576)
2	6.7	6.8	0.6 (576)	6.8	1.0 (576)	6.9	2.5 (576)
3	7.1	7.2	0.8 (576)	7.2	1.7 (576)	7.3	2.1 (576)
4	7.8	7.8	0.9 (576)	7.8	1.2 (576)	7.9	2.1 (576)
5	8.1	8.1	−0.3 (576)	8.1	−0.3 (576)	8.1	0.1 (576)
6	8.3	8.6	3.1 (576)	8.7	4.0 (576)	8.8	5.2 (576)
7	9.1	9.8	8.2 (576)	10.2	11.8 (570)	10.2	12.7 (564)
8	9.4	10.1	7.4 (576)	10.4	10.9 (576)	11.4	21.9 (565)
9	11.1	11.6	4.5 (576)	12.1	8.3 (576)	13.0	16.4 (561)
10	16.9	18.2	7.7 (536)	18.1	7.1 (510)	17.5	3.1 (482)
Mean			3.2*		4.8†		7.8†
SD			2.9		4.2		7.3

*$P < 0.05$.
†$P < 0.005$.
Significant differences between mean B_{max} (mB_{max}) calculated with the polar map method with different filters (PMF) and mean B_{max} calculated with one average time activity curve (mTAC), based on paired Student *t* test.
Number of accepted segments used for calculation of mean B_{max} is indicated in parentheses.

correction factors should be obtained from the ^{11}C-CGP scan itself. However, a new model would have to be developed to achieve this goal, and the introduction of two extra factors (blood volume and tissue fraction) into the model would reduce the precision of all parameters. The choice of 50 pmol/g as an upper limit for the calculated values of B_{max} is arbitrary. However, varying this limit from 25–90 pmol/g did not have much effect, except in volunteer 10. Changing the lower limit for calculation of B_{max} from 0.1–0.01 pmol/g did not affect the number of unacceptable segments, indicating that these were segments in which a B_{max} could not be calculated with the current double-injection method. The high number of segments (40–94) with unreliable values of B_{max} ($\leq$0.1 or $\geq$50 pmol/g) in volunteer 10 might be related to the very high $B_{max(mTAC)}$ (16.9 pmol/g). However, no reasons for the results in this study could be found.

Assessment of Inter-Regional Heterogeneity. Assessment of the spatial distribution of β-adrenoceptor density needs high-quality data. Patient movement between and during scans should be avoided because this can result in considerable artifact. Another factor that should be considered when assessing heterogeneity is the contamination of the myocardial regions by surrounding tissue. The kinetics of ^{11}C-CGP in surrounding tissue will often differ from that in the myocardium, resulting in a differently shaped time-activity curve. In this study, 3 subjects were found with higher values of B_{max} in the inferior region, which could have been caused by spill-over from the liver. An example of this is shown in Figure 2B. To improve the regional measurement of myocardial B_{max} or other parameters being measured, further investigations should focus on techniques to correct for any subject movement between scans and tissue contamination from surrounding tissues like the liver.

The differences found between $B_{max(mTAC)}$ and $B_{max(PMF1/2/3)}$ could occur for two reasons. First, the $B_{max(mTAC)}$ is calculated using the average time-activity curve. This could lead to biased results due to tissue heterogeneity. Because a nonlinear relation exists between the time-activity curve and the calculated value of B_{max}, the average time-activity curve of the whole heart might result in a bias in $B_{max(mTAC)}$. This could explain the differences found in this study (*31*). On the other hand, the polar map approach uses smaller regions to assess regional differences in B_{max}. Smaller regions lead to a lower signal-to-noise ratio, which, because of the nonlinear amplification of the noise signal, could also introduce bias into results (*27*). This study cannot differentiate between the two effects, which may both influence the results. Bias due to heterogeneity could also be present at the regional level. The increasing difference between $B_{max(mTAC)}$ and $B_{max(PMF1/2/3)}$ with decreasing size of segment is possibly more suggestive of a noise, especially considering the (slight) reduction in accepted segments for the less smoothed segments. Additional studies are required to assess the nature of the bias in more detail.

An important issue is which filter or region size should be used for the analysis of cardiac β-adrenoceptor measurement studies. Smaller filters reduce the chance of biased results due to heterogeneity but allow a larger bias due to the

lower signal-to-noise ratios. Larger filters, however, will reduce the chance of regional differences being detected. Because the differences found between whole heart B_{max} and the mean B_{max} of individual areas are negligible compared to the expected differences in cardiac disease, the polar map approach with any of the filters used in this study may be a useful method to assess regional differences. In theory, a direct in vitro validation study would be the best way to assess the polar map approach for regional measurements. However, it is difficult to compare the results from in vitro methods with PET studies, as the former are expressed as pmol/g of protein and the latter as pmol/g of tissue. In addition, receptor densities are environment-dependent and are not necessarily the same in vivo and ex vivo. Nevertheless, Merlet et al. (*18*) have successfully compared changes in receptor density measured using in vitro methods with PET measurements and shown a good correspondence.

CONCLUSION

This study has demonstrated that the parametric polar map method is a feasible approach for assessing regional variations in B_{max}. This method should be useful in the investigation of cardiac diseases in which a regional variation in β-adrenoceptor density may be expected, e.g., ischemic heart disease and arrythmogenic cardiomyopathies.

ACKNOWLEDGMENTS

The authors are grateful to the radiographers and the members of the MRC Cyclotron Unit Department of Radiochemistry for their help with scanning and the preparation of the radioligand ^{11}CGP 12177. Richard M. de Jong was supported by a grant from the Dutch Heart Foundation.

REFERENCES

1. Lathers CM, Spivey WH, Levin RM. The effect of chronic timolol in an animal model for myocardial infarction. *J Clin Pharmacol*. 1988;28:736–745.
2. Brodde OE. Beta 1- and beta 2-adrenoceptors in the human heart: properties, function, and alterations in chronic heart failure. *Pharmacol Rev*. 1991;43:203–242.
3. Bristow MR, Ginsburg R, Umans V, et al. $Beta_1$- and $beta_2$-adrenergic-receptor subpopulations in nonfailing and failing human ventricular myocardium: coupling of both receptor subtypes to muscle contraction and selective $beta_1$-receptor down-regulation in heart failure. *Circ Res*. 1986;59:297–309.
4. Maisel AS, Motulsky HJ, Insel PA. Externalization of β-adrenergic receptors promoted by myocardial ischemia. *Science*. 1985;230:183–186.
5. Bristow MR, Anderson FL, Port JD, et al. Differences in beta-adrenergic neuroeffector mechanisms in ischemic versus idiopathic dilated cardiomyopathy. *Circulation*. 1991;84:1024–1031.
6. Brodde OE, Zerkowski HR, Doetsch N, Motomura S, Khamssi M, Michel MC. Myocardial β-adrenoceptor changes in heart failure: concomitant reduction in β_1 and β_2-adrenoceptor function related to the degree of heart failure in patients with mitral valve disease. *J Am Coll Cardiol*. 1989;14:323–331.
7. Yamada S, Ishima T, Tomita T, Hayashi T, Okada T, Hayashi E. Alterations in cardiac α- and β-adrenoceptors during the development of spontaneous hypertension. *J Pharmacol Exp Ther*. 1984;228:454–459.
8. Heyliger CE, Pierce GN, Singal PK, Beamish RE, Dahalla NS. Cardiac α- and β-adrenergic receptor alterations in diabetic cardiomyopathy. *Basic Res Cardiol*. 1982;77:610–618.
9. Lefkowitz RJ, Caron MG, Stiles GL. Mechanism of membrane-receptor regulation. Biochemical, physiological and clinical insights derived from studies of the adrenergic receptors. *N Engl J Med*. 1984;24:1570–1579.
10. Maisel AS, Phillips C, Michel MC, Ziegler MG, Carter SM. Regulation of cardiac β-adrenergic receptors by captopril. Implications for congestive heart failure. *Circulation*. 1989;80:669–675.
11. Levett JM, McGrath LB, Bianchi JM. Beta receptor derangement in postinfarction left ventricular perianeurysm tissue. *Clin Cardiol*. 1991;14:909–912.
12. Allman KC, Stevens MJ, Wieland DM, et al. Noninvasive assessment of cardiac diabetic neuropathy by carbon-11 hydroxy ephedrine and positron emission tomography. *J Am Coll Cardiol*. 1993;22:1425–1432.
13. Kaye MP, Randall WC, Hageman GR, Geis WP, Priola DV. Chronology and mode of reinnervation of the surgically denervated canine heart. Functional and chemical correlates. *Am J Physiol (Heart Circ Physiol)*. 1977;2(suppl):H431–H437.
14. Schwaiger M, Hutchins GD, Kalff V, et al. Evidence for regional catecholamine uptake and storage in the transplanted human heart by positron emission tomography. *J Clin Invest*. 1991;87:1681–1690.
15. Camici PG, Rosen SD. Does positron emission tomography contribute to the management of clinical cardiac problems? *Eur Heart J*. 1996;17:174–181.
16. Delforge J, Syrota A, Lancon JP, et al. Cardiac beta-adrenergic receptor density measured in vivo using PET, CGP 12177, and a new graphical method. *J Nucl Med*. 1991;32:739–748.
17. Delforge J. Correction of a relationship that assesses beta-adrenergic receptor concentration with PET and Carbon-11-CGP 12177 [letter]. *J Nucl Med*. 1994;35:921.
18. Merlet P, Delforge J, Syrota A, et al. Positron emission tomography with ^{11}C CGP-12177 to assess beta-adrenergic receptor concentration in idiopathic dilated cardiomyopathy. *Circulation*. 1993;87:1169–1178.
19. Lefroy DC, de Silva R, Choudhury L, et al. Diffuse reduction of myocardial beta-adrenoceptors in hypertrophic cardiomyopathy: a study with positron emission tomography. *J Am Coll Cardiol*. 1993;22:1653–1660.
20. Anthonio RL, van Waarde A, Willemsen ATM, et al. Experimental and clinical beta receptor studies. In: Blanksma PK, Niemeyer MG, Paans AMJ, van der Wall EE, eds. *Cardiac PET*. Boston, MA: Kluwer Academic Publishers; 1995:201–210.
21. Choudhury L, Guzzetti S, Lefroy DC, et al. Myocardial β adrenoceptors and left ventricular function in hypertrophic cardiomyopathy. *Heart*. 1996;75:50–54.
22. Rosen SD, Boyd H, Rhodes CG, Kaski JC, Camici PG. Myocardial β-adrenoceptor density and plasma catecholamines in Syndrome X. *Am J Cardiol*. 1996;78:37–43.
23. Choudhury L, Rosen SD, Lefroy DC, Nihoyannopoulos P, Oakley CM, Camici PG. Myocardial beta adrenoceptor density in primary and secondary left ventricular hypertrophy. *Eur Heart J*. 1997;18:108–116.
24. Rhodes CG, Wollmer P, Fazio F, Jones T. Quantitative measurement of regional extravascular lung density using positron emission and transmission tomography. *J Comput Assist Tomogr*. 1981;5:783–791.
25. Iida H, Rhodes CG, de Silva R, et al. Myocardial tissue fraction: correction for partial volume effects and measure of tissue viability. *J Nucl Med*. 1991;32:2169–2175.
26. Blanksma PK, Willemsen ATM, Meeder JG, et al. Quantitative myocardial mapping of perfusion and metabolism using parametric polar map displays in cardiac PET. *J Nucl Med*. 1995;36:153–158.
27. Lammertsma AA, de Silva R, Araujo LI, Jones T. Measurement of regional myocardial blood flow using $C^{15}O_2$ and positron emission tomography: comparison of tracer models. *Clin Phys Physiol Meas*. 1992;13:1–20.
28. De Jong RM, Blanksma PK, Willemsen ATM, et al. Posterolateral defect of the normal human heart investigated with nitrogen-13-ammonia and dynamic PET. *J Nucl Med*. 1995;36:581–585.
29. Iida H, Takahashi A, Tamura Y, Ono Y, Lammertsma AA. Myocardial blood flow: comparison of oxygen-15-water bolus injection, slow infusion and oxygen-15-carbon dioxide slow inhalation. *J Nucl Med*. 1995;36:78–85.
30. Hermansen F, Rosen SD, Fath-Ordoubadi F, et al. Measurement of myocardial blood flow with oxygen-15 labeled water: comparison of different administration protocols. *Eur J Nucl Med*. 1998;25:751–759.
31. Blomqvist G, Lammertsma AA, Mazoyer B, Wienhard K. Effect of tissue heterogeneity on quantification in positron emission tomography. *Eur J Nucl Med*. 1995;22:652–663.